

**Supplementary Table 1. Effects of *Chaer* knockout on heart function.** WT, wildtype; KO, knockout; HR, heart rate; IVSs,d, ystolic and diastolic interventricular septum; LVDs,d, systolic and diastolic left ventricular dimension; LVPWs,d, left vetricular posterior wall thickness; EF, ejection fraction; FS, fraction shortening; Data were mean  $\pm$  s.e.m. Sample numbers were labeled after each group item. \* $P < 0.05$ , \*\*\* $P < 0.001$  versus WT; # $P < 0.05$ , ## $P < 0.01$ , ### $P < 0.001$  versus corresponding Sham groups (Students'  $t$  test).

	Sham		TAC			
	WT (8)	KO (6)	WT (10)		KO (7)	
Body weight (g)	26.4 $\pm$ 0.3	26.4 $\pm$ 0.4	27.0 $\pm$ 0.3		26.9 $\pm$ 0.3	
Heart weight (mg)	109.1 $\pm$ 2.1	111.2 $\pm$ 1.4	158.2 $\pm$ 1.5	###	134.6 $\pm$ 1.4	### ***
Lung weight (mg)	130.4 $\pm$ 2.8	131.7 $\pm$ 2.1	162.2 $\pm$ 1.6	###	144.9 $\pm$ 1.6	### ***
HR (bpm)	475.5 $\pm$ 5.9	479.7 $\pm$ 7.2	486.5 $\pm$ 6.6		477.9 $\pm$ 7.4	
IVSd (mm)	0.65 $\pm$ 0.01	0.66 $\pm$ 0.01	0.73 $\pm$ 0.01	###	0.71 $\pm$ 0.01	
LVDd (mm)	3.75 $\pm$ 0.04	3.81 $\pm$ 0.03	4.11 $\pm$ 0.03	###	3.89 $\pm$ 0.03	# ***
LVPWd (mm)	0.64 $\pm$ 0.01	0.65 $\pm$ 0.01	0.74 $\pm$ 0.01	###	0.69 $\pm$ 0.01	## *
IVSs (mm)	1.03 $\pm$ 0.01	1.01 $\pm$ 0.01	1.15 $\pm$ 0.02	###	1.08 $\pm$ 0.01	## ***
LVDs (mm)	1.98 $\pm$ 0.03	2.02 $\pm$ 0.02	2.64 $\pm$ 0.03	###	2.17 $\pm$ 0.01	### ***
LVPWs (mm)	1.01 $\pm$ 0.01	1.04 $\pm$ 0.01	1.15 $\pm$ 0.02	###	1.09 $\pm$ 0.02	# ***
EF (%)	80.6 $\pm$ 1.3	80.8 $\pm$ 1.1	71.2 $\pm$ 0.6	###	77.3 $\pm$ 0.6	# ***
FS (%)	47.4 $\pm$ 0.6	47.0 $\pm$ 0.5	35.8 $\pm$ 0.6	###	44.0 $\pm$ 0.5	## ***

**Supplementary Table 2. List of genes oppositely affected by PE and Chaer deficiency.**  
 Values are fold change (> 1.5 folds) in log<sub>2</sub> scale. Highlighted are the genes reported to be related to cardiomyopathy.

Gene ID	siChaer-siNeg	siChaer PE-siChaer
PLA2G7	0.902427	-1.47485
NRTN	0.853064	-1.27416
OSGIN1	0.826706	-1.25789
H1FX	0.595154	-1.11182
GJA5	1.010547	-1.11063
RIL	0.947315	-1.09966
RCOR2L1	0.740647	-1.04932
NTN1	0.640203	-1.02148
PPP1R35	0.679942	-0.96964
SLC25A10	0.660916	-0.91796
NNAT	0.597051	-0.91062
RPL39	0.742797	-0.85096
HADH	0.616153	-0.84224
CDC20	1.172966	-0.8403
KIF20A	1.059816	-0.80736
NUSAP1	0.800234	-0.76332
TESC	1.040555	-0.76324
FAM102A	0.774076	-0.74836
ASF1B	0.775737	-0.7482
CDKN2C	1.03606	-0.7439
PLK1	1.093322	-0.74111
TEAD2	0.644916	-0.73905
MRI1	0.700758	-0.7262
HAUS4	0.676757	-0.72576
GMEB1	0.62528	-0.7188
TRIB1	0.708525	-0.7152
RPL38	0.604318	-0.71396
GSTM1	0.941065	-0.70755
RRM2	1.106673	-0.70729
SPC24	0.70323	-0.70684
MGMT	0.894608	-0.70526
HINT2	0.641423	-0.70117
FAM57B	0.958901	-0.68031
GTSE1	0.846868	-0.67046
RPS29	0.589362	-0.67007
RAE1	0.803523	-0.65785
KCNJ12	0.859557	-0.6548
MELK	0.624382	-0.65403

---

PALM	0.709485	-0.65287
PTOV1	0.737124	-0.64689
TCEAL7	0.909581	-0.64196
DAPK1	0.875446	-0.6349
CDCA3	1.173644	-0.62509
<b>IQGAP3</b>	<b>0.771085</b>	<b>-0.62395</b>
INO80B	0.773002	-0.6218
CKAP2	0.686529	-0.62008
TROAP	0.783586	-0.61694
<b>AKAP1</b>	<b>0.5875</b>	<b>-0.61553</b>
<b>PTTG1</b>	<b>1.165298</b>	<b>-0.61481</b>
KIF18B	0.879716	-0.60351
FAM100B	0.814713	-0.59648
<b>LYRM4</b>	<b>0.706861</b>	<b>-0.59623</b>
PHLDB1	0.664525	-0.59437
<b>FOXM1</b>	<b>0.946475</b>	<b>-0.5912</b>
PALD1	0.703006	-0.586
<b>CCL20</b>	<b>-1.35475</b>	<b>2.436636</b>
<b>KIF5B</b>	<b>-0.94106</b>	<b>2.378966</b>
IFIT1LB	-1.71041	2.008517
<b>SEMA3C</b>	<b>-0.81381</b>	<b>1.774554</b>
<b>UTRN</b>	<b>-0.80677</b>	<b>1.606805</b>
<b>ENO3</b>	<b>-0.83967</b>	<b>1.53494</b>
SNTB1	-0.68555	1.495425
<b>BCL2</b>	<b>-0.61098</b>	<b>1.34939</b>
<b>RXFP1</b>	<b>-0.63707</b>	<b>1.316754</b>
<b>ACSL4</b>	<b>-0.6021</b>	<b>1.307842</b>
B3GALT2	-0.61564	1.263892
RIF1	-0.69967	1.105045
<b>RGS2</b>	<b>-0.71724</b>	<b>1.100427</b>
PRRG4	-0.95495	1.092152
ATP13A3	-0.66171	1.082246
NFKBIZ	-0.6688	1.081044
<b>STC1</b>	<b>-0.8586</b>	<b>1.064101</b>
CAPN12	-0.58912	1.052798
<b>NEBL</b>	<b>-0.90671</b>	<b>0.978596</b>
TSPAN2	-0.85819	0.924806
<b>PRKG1</b>	<b>-0.82525</b>	<b>0.906017</b>
<b>KRAS</b>	<b>-0.7776</b>	<b>0.898436</b>
MIR761	-0.69176	0.875956
<b>HOMER1</b>	<b>-0.7917</b>	<b>0.873153</b>
FAM174B	-0.64802	0.865487
CCDC88A	-0.91491	0.850827

---

---

HLTF	-0.7316	0.848301
DCUN1D1	-0.9275	0.843988
<b>ROCK1</b>	<b>-0.81605</b>	<b>0.834311</b>
C1GALT1	-0.91229	0.828817
ARFGEF1	-0.86806	0.825254
RGS7BP	-0.62727	0.785792
ATRX	-0.94468	0.784108
<b>SGCD</b>	<b>-0.63839</b>	<b>0.773244</b>
PANK3	-0.60505	0.771385
ASCC3	-0.88859	0.74602
<b>EEA1</b>	<b>-0.66632</b>	<b>0.74278</b>
YES1	-0.90094	0.73757
TMEM47	-0.83169	0.733422
<b>RASA1</b>	<b>-1.14443</b>	<b>0.728101</b>
PPM1K	-1.01437	0.714557
PICALM	-0.62073	0.712595
TMED5	-0.76787	0.710244
SETD7	-1.20941	0.7009
MYO9A	-0.9248	0.700796
<b>TRPM7</b>	<b>-0.80302</b>	<b>0.695232</b>
<b>TGFBR1</b>	<b>-0.69314</b>	<b>0.694994</b>
TROVE2	-1.29791	0.685457
HIST2H4	-1.19967	0.681722
<b>TRDN</b>	<b>-0.84643</b>	<b>0.677743</b>
ACBD5	-0.8883	0.675817
CD2AP	-0.74938	0.673106
HTATSF1	-0.75704	0.662329
LMBRD2	-0.64633	0.65909
HNRPH1	-1.01218	0.658643
SPCS3	-0.65497	0.658064
TAOK1	-1.33803	0.650267
UPRT	-0.71241	0.648604
<b>GADD45A</b>	<b>-0.59812</b>	<b>0.647708</b>
ABCB7	-0.68236	0.646996
FAM198B	-0.62271	0.646304
ESF1	-0.85132	0.644565
<b>MSRA</b>	<b>-0.62384</b>	<b>0.64304</b>
SNRPF	-0.70603	0.642973
<b>DNM1L</b>	<b>-0.62562</b>	<b>0.642736</b>
RC3H2	-0.64278	0.641938
OXCT1	-0.64493	0.634186
IFT74	-0.78369	0.633527
2310002L09RIK	-1.28327	0.632601

---

---

ZDHHC21	-0.736	0.622869
PRPF39	-0.84193	0.622213
D14ABB1E	-0.75236	0.620744
EDEM3	-0.80372	0.619399
<b>HSP90AA1</b>	<b>-0.66241</b>	<b>0.617907</b>
<b>KRIT1</b>	<b>-0.63832</b>	<b>0.614043</b>
DMXL1	-1.18488	0.612833
MAN1A2	-0.72617	0.607662
CDC42BPA	-0.61032	0.605495
SMEK2	-0.96949	0.602348
COPS2	-0.83891	0.600305
MPP5	-0.6246	0.596393
NIPBL	-0.91084	0.595067
<b>TECRL</b>	<b>-1.09286</b>	<b>0.595032</b>
<b>PPP3CA</b>	<b>-0.9464</b>	<b>0.59363</b>
RANBP2	-0.75785	0.590086
<b>PROS1</b>	<b>-0.64417</b>	<b>0.589844</b>

---

**Supplementary Table 3. Gene ontology analysis for negatively correlated genes between PE induction and *Chaer* deficiency in NRVM.**

<b>Functional Clusters</b>	<b>Count</b>	<b>Percentage</b>	<b><i>P</i>-Value</b>	<b>Benjamini</b>
mitotic cell cycle	12	8.9	8.30E-07	7.70E-04
cell cycle	16	11.9	1.60E-05	4.80E-03
organelle fission	9	6.7	6.00E-05	9.20E-03
nuclear division	9	6.7	4.70E-05	1.10E-02
ribonucleotide binding	25	18.5	3.90E-04	1.30E-02
ATP binding	23	17	1.10E-04	2.30E-02
cytoskeleton organization	10	7.4	3.90E-04	4.40E-02

**Supplementary Table 4. Top down-regulated genes show a property being clustered in conserved transcriptional loci.** 27 out of top 50 down-regulated genes after *Chaer* KD are clustered in 11 genomic transcription loci while none of top 50 up-regulated genes can be clustered to any co-regulated genomic loci.

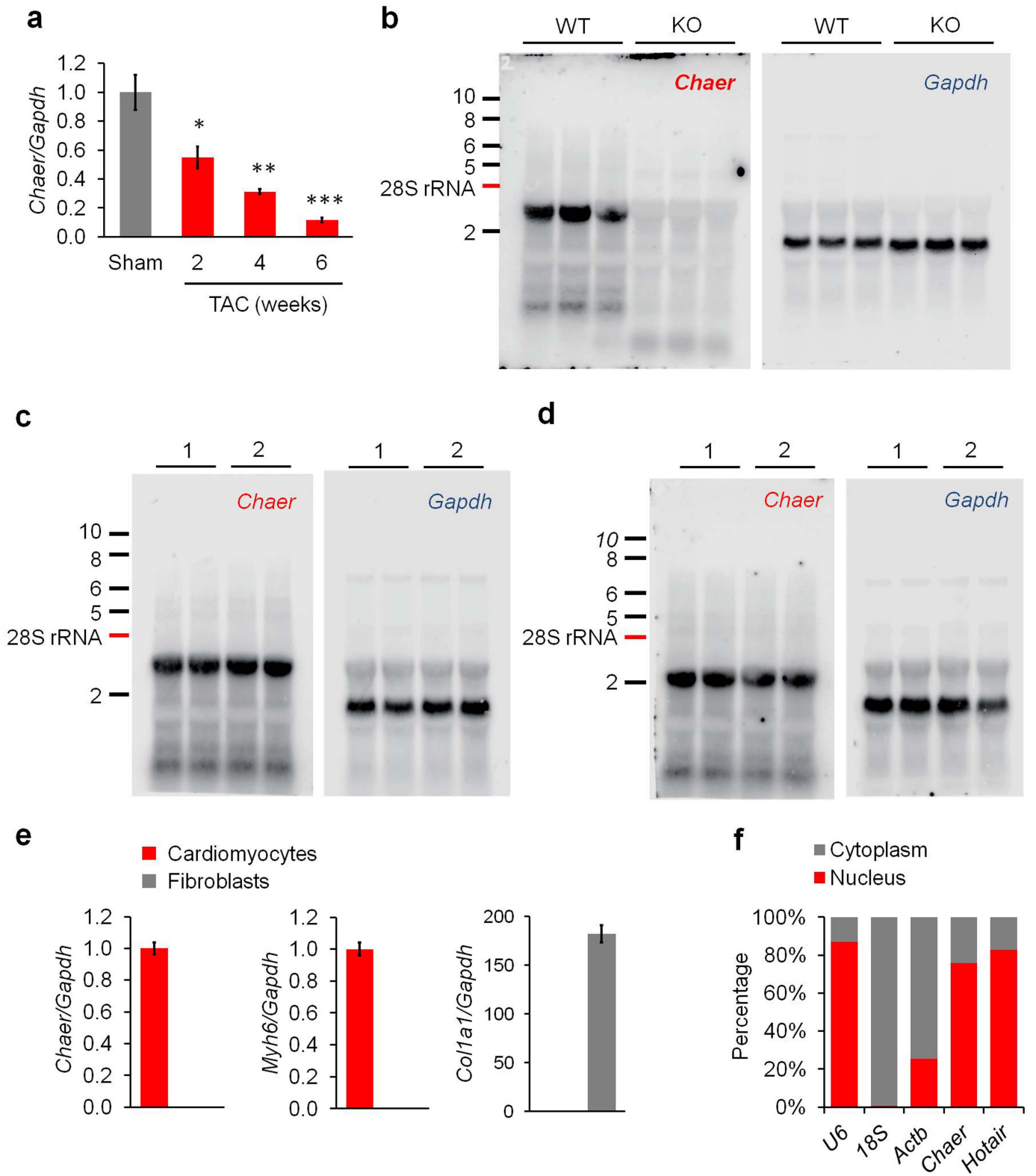
Clusters	Genes	Regulation	Mouse	Rat	Human
1	H19, Igf2	Down	chr7	chr1	chr11
2	Gbp1, Gbp2, Gbp5, Gbp7	Down	chr3	chr2	chr1
3	Isg15, Agrn	Down	chr4	chr5	chr1
4	Oas11, Oasl2	Down	chr5	chr12	chr12
5	Cxcl3, Cxcl5, Pf4,	Down	chr5	chr14	chr4
6	Ccl2, Ccl7, Ccl12	Down	chr11	chr10	chr17
7	ssh2, coro6, Taok1	Down	chr11	chr10	chr17
8	Rsad2, Cmpk2	Down	chr12	chr6	chr2
9	Mx1, Mx2, Bace2	Down	chr16	chr11	chr21
10	Rtp4, Masp1	Down	chr16	chr11	chr3
11	Ifit1, Ifit2, Ifit3, Ifit11b	Down	chr19	chr1	chr10

**Supplementary Table 5. Primer list.**

Genes	Species	Purpose	Sense (5'→3')	Anti-sense (5'→3')
Chaer	mouse	qPCR	TCCAATGAGGGAAGCGAAGC	GTCCGATGCCAGTTCCAGTT
	rat	qPCR	GTAGACTGCTTGAGGGAACAG	AGGAGGTGTAGGATCTGCAGA
	mouse	cloning	AATGCGGCCGCCTCACGGAGT GCAGACTC	AGGAAGCTTCCACAGTAGGCC TGAGAGCT
	human	cloning	GGAAACACTTCAGCTATGACA	GCCAGGCTCTTCGGGGCTT
		qPCR (pair 1)	GAGCCAAAAACCAACAAGGA	GGCCCAGCTACTGTGCTAAC
		qPCR (pair 2)	GTGAAGGAACAGGGTGTGCT	GCCCAGCTACTGTGCTAACC
Chaer-66mer	mouse	cloning	TTTGGATCCTCACGGAGTGCAG ACTCGGT	AGAGATATCCATCGGACACGT GTTACCA
Hotair	mouse	qPCR	CTTTCAAGGCCTGTCTCCTG	CAACATTCTAGCTGCACGGA
	rat	qPCR	CATGACCAGCGATCTGACCAC	CAGTGCACCTCACATCTGCAGA
	mouse	cloning	CAGGATATCACAGTGGAAAGGA AGGAAAGAATCA	CAGCTCGAGGCATTTGTAAGC AAGGCTTTCA
Hotair-89mer	mouse	cloning	TTTGGATCCATACTAGCTTTTC CACACCCA	TTTGGATCCATACTAGCTTTTC CACACCCA
Hottip	mouse	qPCR	GCACCATTCACTCACACTCCTG	CAAAACGGAATGCAACAGTG GA
Fendrr	mouse/ rat	qPCR	GTGAGACCCGAGAGGCTGGA	GAAGATGGTCCAGCGCCCACT
H19	mouse	qPCR	CCTCAGACGGAGATGGACGA	CCCCCTTTTGAATTTGCACTA
	rat	qPCR	GATGACAGGTGTGGTCAACG	CAGACATGAGCTGGGTAGCA
	rat	AciI	CCATACTGTGCCTCTGGTTG	TGGGTGCTCCTCACTGTCAC
	rat	AciI/ChI P	CTATATGTTCTCGACCTCAA	CCAGCGCACGTTTCGCCTCAC
	rat	AciI	GTCCTTGTACTGATTGGTTG	CCTCCCACACCCGGTGCTTC
Anf	mouse	qPCR	GTACAGTGCGGTGTCCAACA	TCTCCTCCAGGTGGTCTAGCA
	rat	qPCR	ATACAGTGCGGTGTCCAACA	AGCCCTCAGTTTGCTTTTCA
	human	qPCR	TCTGCCCTCCTAAAAAGCAA	ATCACAACTCCATGGCAACA
	mouse	ChIP	ATCGCTTTATCGCTGCAAGT	TCAGCTTTTGTCCGTCCTG
	rat	ChIP	GAGGCCAATGAATCAGGTGT	TGTCAGGGGCTCCAAATAAG
Myh7	mouse	qPCR	GTACAGCTCTTCTACAGGCCT	GGCACAAAAACATCTTTCTTG AGG
	rat	qPCR	GCTCCTAAGTAATCTGTTTGC	AAGTGAGGGTGCCTGGAGCG
	human	qPCR	TGTGCTCGCCAGAATGGAGTA	CAGCGCTCCTCAGCATCTGCC
	mouse	ChIP	ACTCAGACCCTGAACATGCC	ACCCAGTCCCTAGCCAGATT

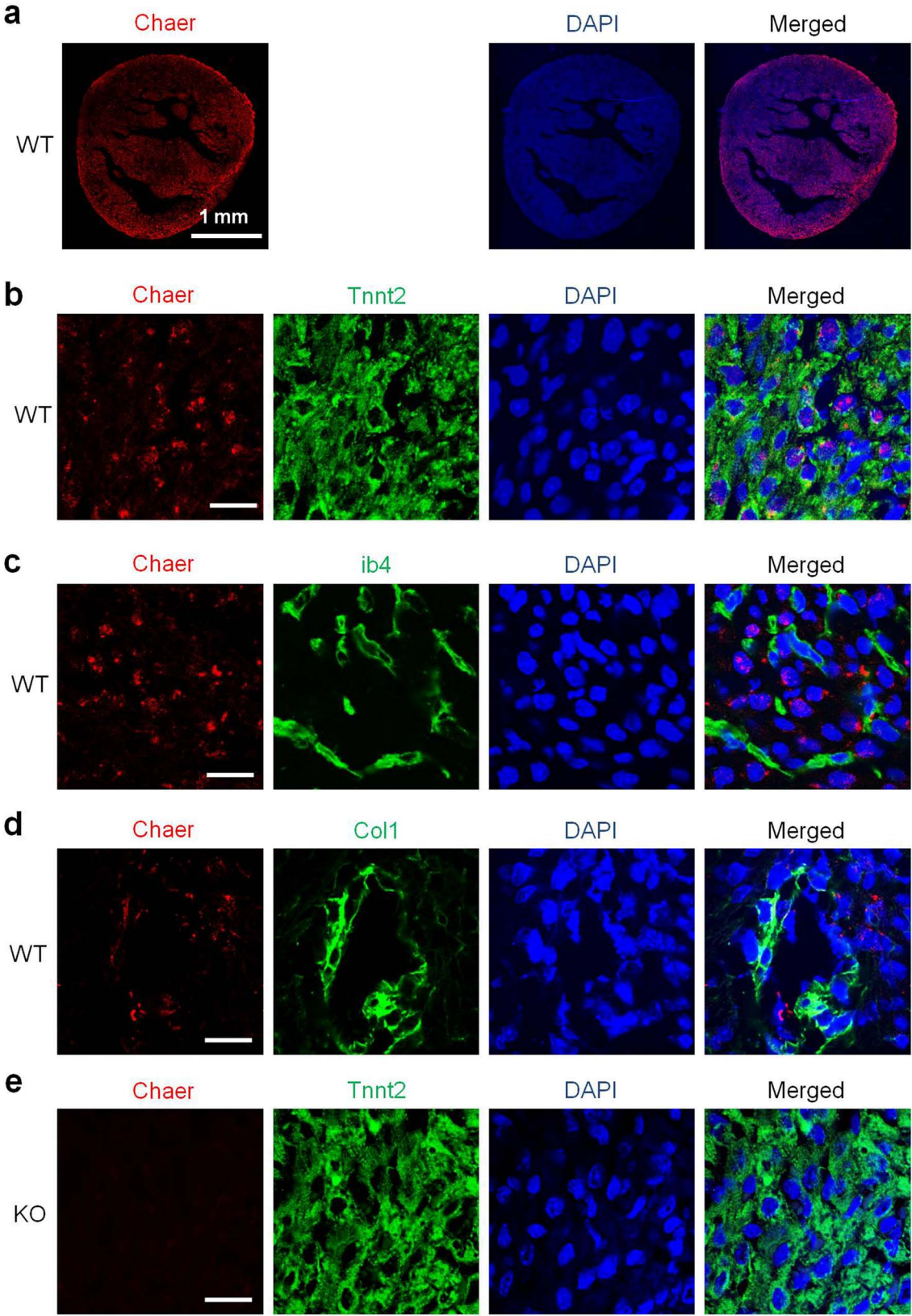


	rat	ChIP	CGTGGCTCAAAGAAAGGAAG	TCAGCACGTGGAAGAGTGAC
Acta1	mouse/rat	qPCR	GCTGTGTTCCCATCCATCGT	GCAGGCACGTTGAAGGTCTC
	human	qPCR	TGCCCATTTATGAGGGCTAC	GCCATCTCGTTCTCGAAGTC
	mouse	ChIP	AGCAGTCTGCAAAGCAGTGA	GACCAGGCCGTATATGGAGA
Gata4	rat	ChIP	CTCCCCTCACTACCTCCTCC	AAGCTCCCCAATCCAGAGAT
	mouse	qPCR	TCTCACTATGGGCACAGCAG	GCGATGTCTGAGTGACAGGA
	rat	qPCR	TCTCACTATGGGCACAGCAG	CGAGCAGGAATTTGAAGAGG
Hopx	rat	ChIP	CTTCTCCTCTACCAGCCACG	TCTCTCGGGGAATGAAAGTG
	rat	qPCR	AACAAGGTCAACAAGCACCC	CCACAGGAGGAGAAAGCAAG
	mouse/rat	qPCR	TCCTGCACCACCAACTGCTTAG	GATGACCTTGCCACAGCCTTG
Gapdh	human	qPCR	GAGTCAACGGATTTGGTCGT	TTGATTTTGGAGGGATCTCG
	mouse	ChIP	GAATGCCTTTTCTCCCTTCC	GAGCCAGGGACTCTCCTTTT
	rat	ChIP	TTTCTGGTTTCTGGGTCTG	ATGAGGGTTCCAGGATAGG
U6	mouse	qPCR	GTGCTCGCTTCGGCAGCA	GGAACGCTTCACGAATTTGC
Rn18S	mouse	qPCR	TATGGTTCCTTTGGTCGCTCG	GATCTGATAAATGCACGCATCC
Actb	mouse/rat	qPCR	GGAGCACCTGTGCTGCTCA	GCCAGGTCCAGACGCAGGAT
Cola1	mouse	qPCR	AGGCATAAAGGGTCATCGTG	ACCGTTGAGTCCATCTTTGC
Ezh2	mouse	cloning	ACAGGATCCATGGGCCAGACT GGGAAGAA	ATTCTCGAGTCAAGGGATTTCC CATTTCTCGTTCGA
Chaer D2166-2737	mouse	cloning	TCTGGATCCGCCTCACGGAGTG CAGACTC	TAACTCGAGCTGTCCCAGTAC CTCACACC
Chaer D1666-2737	mouse	cloning	TCTGGATCCGCCTCACGGAGTG CAGACTC	TAACTCGAGCTCCCTCTTTCT CATTTGC
Chaer D1059-2737	mouse	cloning	TCTGGATCCGCCTCACGGAGTG CAGACTC	TAACTCGAGATGCCGGACCCT TCTACTCT
Chaer D525-2737	mouse	cloning	TCTGGATCCGCCTCACGGAGTG CAGACTC	TAACTCGAGTGAGCGCTGTGG AACACAGC
Chaer D0-505	mouse	cloning	AGTGGATCCGGTGTGAGGTACT GGGACAG	TAACTCGAGCCACAGTAGGCC TGAGAGCT
Chaer D0-1039	mouse	cloning	AGTGGATCCGCAAATGAGGAA AGAGGGAG	TAACTCGAGCCACAGTAGGCC TGAGAGCT
Chaer D0-1646	mouse	cloning	TCTGGATCCAGAGTAGAAGGG TCCGGCAT	TAACTCGAGCCACAGTAGGCC TGAGAGCT
Chaer D0-2146	mouse	cloning	TCTGGATCCGCTGTGTTCCACA GCGCTCA	TAACTCGAGCCACAGTAGGCC TGAGAGCT



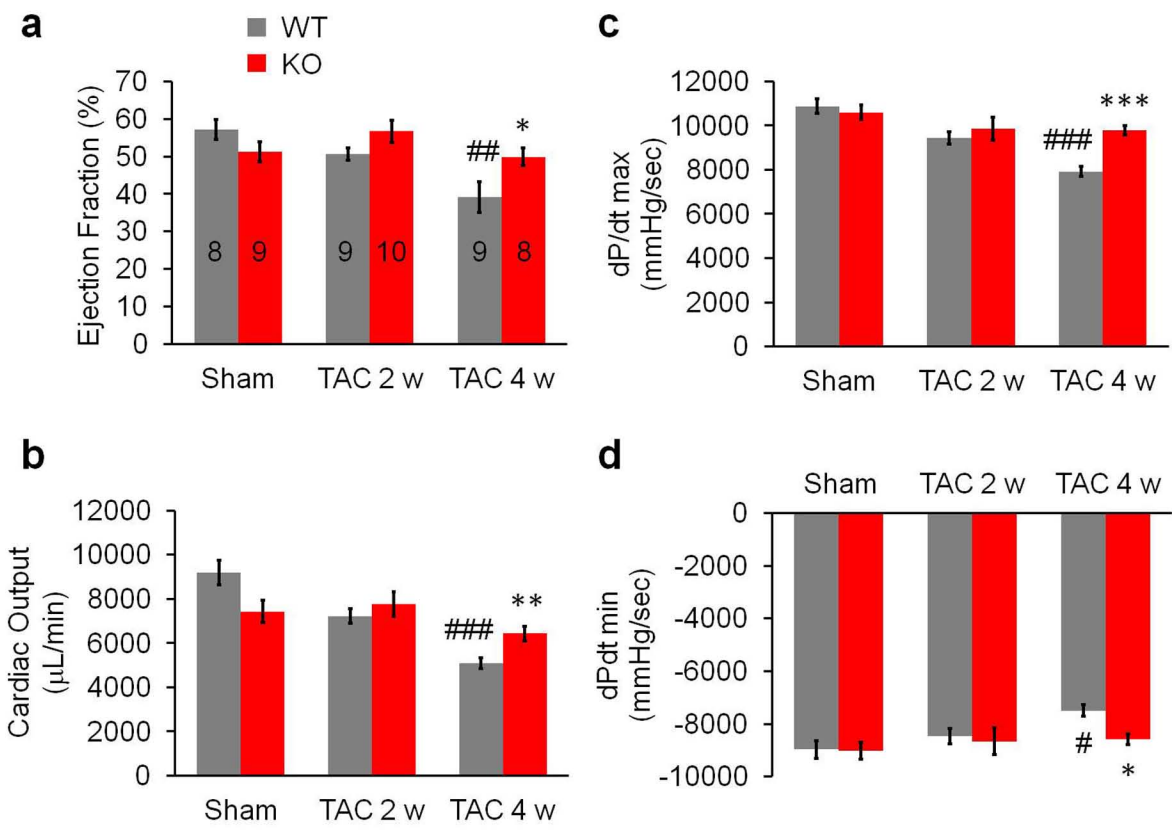
**Supplementary Figure 1. Characterization of *Chaer* expression in mouse.**

(a) RT-PCR for *Chaer* expression in mouse hearts at 2, 4 and 6 weeks after transaortic constriction (TAC) surgery. Data were mean  $\pm$  s.e.m. n =4. \* $P < 0.05$ , \*\*  $P < 0.01$ , \*\*\*  $P < 0.001$  versus sham (Students'  $t$  test). (b) Northern blot analysis for *Chaer* and glyceraldehyde 3-phosphate dehydrogenase (*Gapdh*) in wild-type (WT) and *Chaer* knockout (KO) mouse hearts. (c) Northern blot analysis in rat hearts detected a single band of *Chaer* transcript with a size at 2.7 kb. (d) Northern blot analysis in normal human hearts detected a single band of *Chaer* transcript with a size around 2 kb. (e) RT-PCR for expression of *Chaer*, *Myh6* (alpha-myosin heavy chain 6, marker for cardiomyocytes), and *Colla1* (collagen, type I, alpha 1, marker for fibroblasts) in sorted cardiomyocytes and cardiac fibroblasts from adult mouse heart. Data were mean  $\pm$  S.D from triplicates. (f) Subcellular localization of *Chaer* and *Hotair* detected by real-time RT-PCR in cytosol and nuclear fractions from mouse heart. *U6* RNA was used as a nuclear RNA marker, while *18S* and *Actb* (actin, beta) were used as cytosol RNA markers.



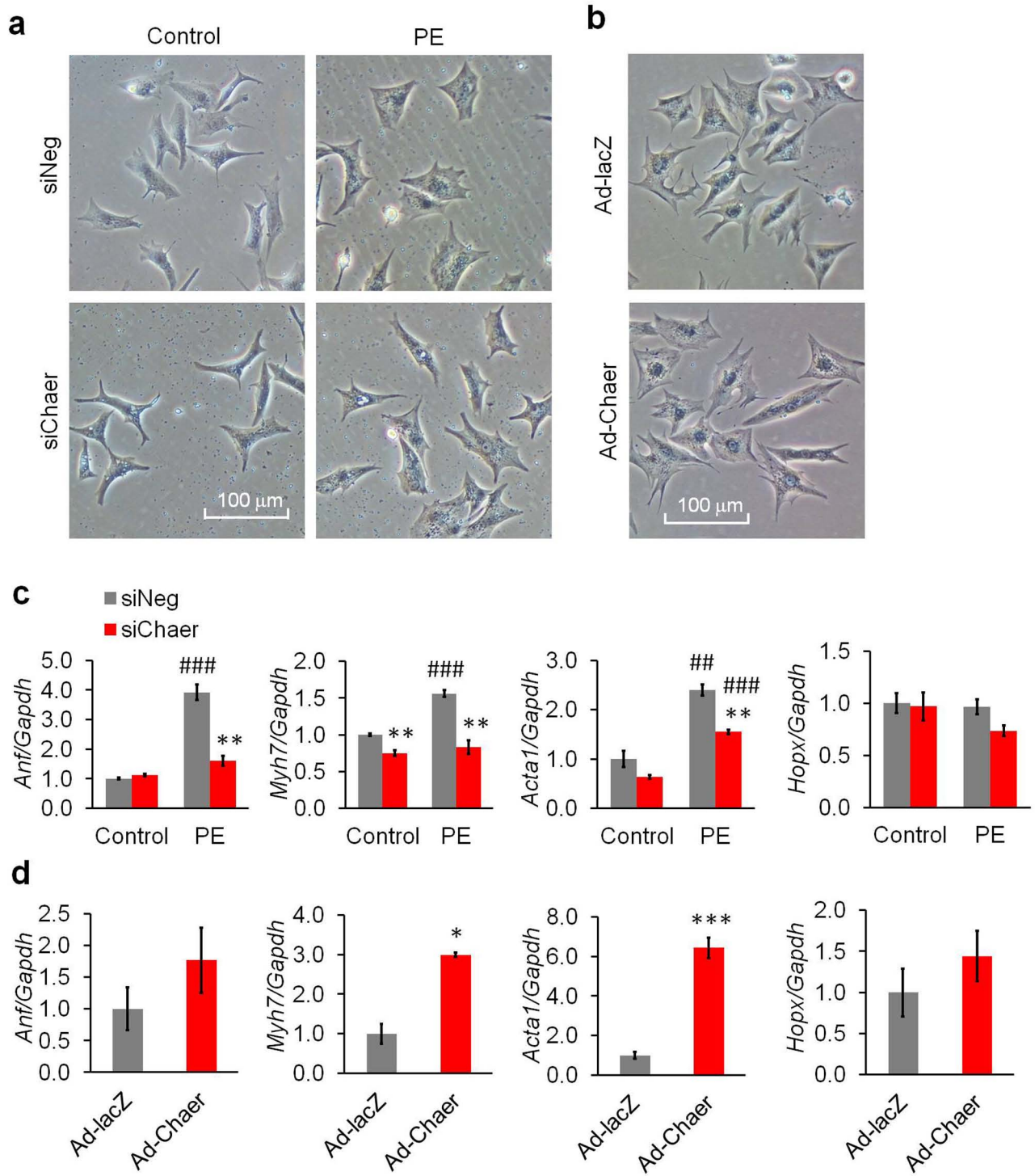
**Supplementary Figure 2. Characterization of *Chaer* in mouse heart.**

**(a-d)** RNA fluorescent in situ hybridization (FISH) assay to visualize *Chaer* in heart of 7-day old mice at large scale **(a)** and small scale **(b-d)**, as well as to specify the cells expressing *Chaer* using markers including Troponin T type 2 (*Tnnt2*) for cardiomyocytes **(b)**, isolectin b4 (*ib4*) for epithelial cells **(c)** and collagen 1 (*Col1*) for a fibroblasts **(d)**. Scale bar **(b-d)**, 20  $\mu\text{m}$ .



**Supplementary Figure 3. Hemodynamics of cardiac function in wild-type and *Chaer* knockout hearts during TAC-induced hypertrophy.**

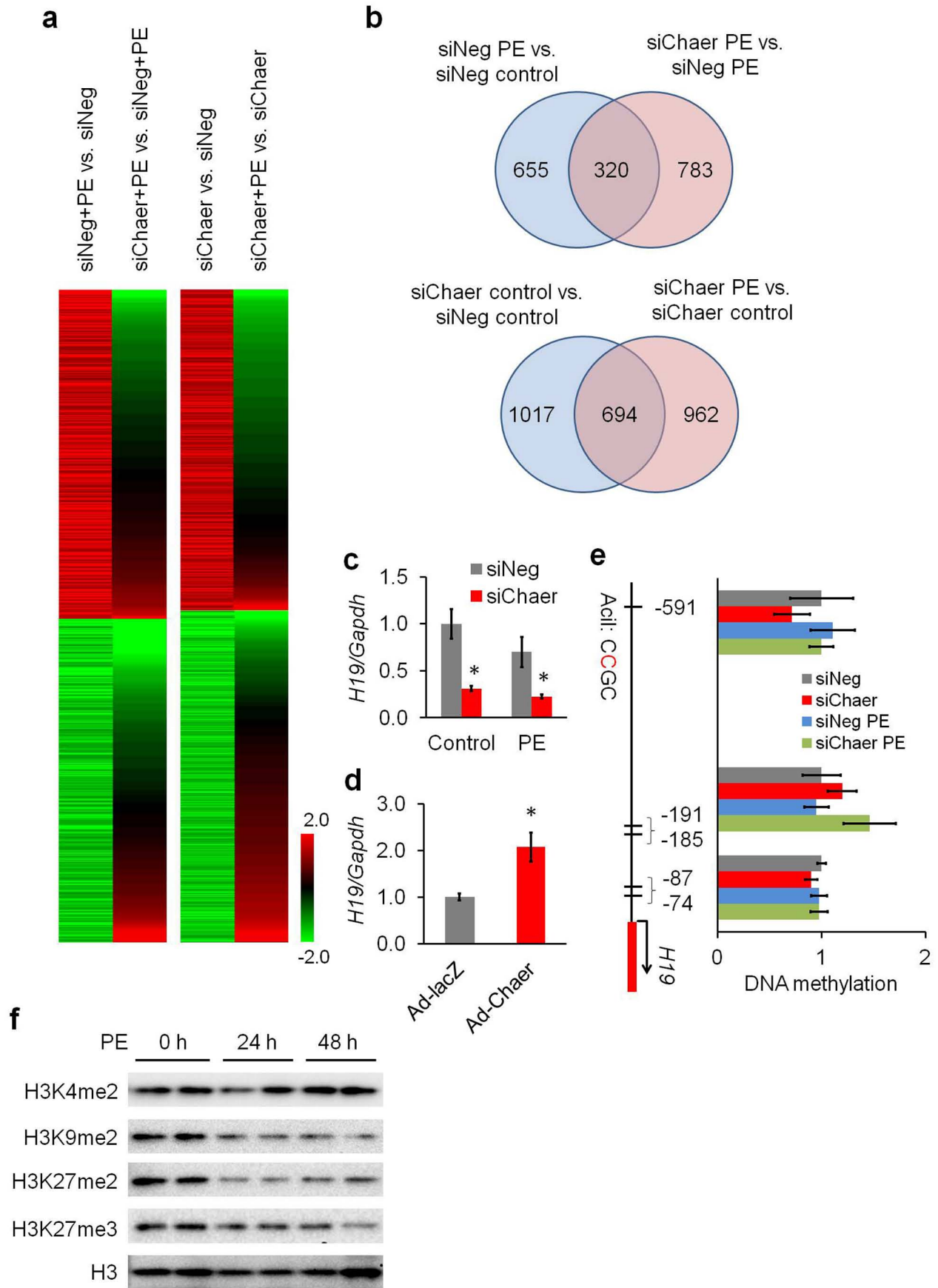
(a-d) Cardiac contractility based on pressure-volume (PV) loop measurements collected before, 2 weeks and 4 weeks after transaortic constriction (TAC) surgery in wild-type (WT) and *Chaer* knockout (KO) mice. (a) Ejection fraction. (b) Cardiac output. (c) Maximum dp/dt. (d) Minimum dp/dt. Data were mean  $\pm$  s.e.m. Sample numbers were labeled on bars in panel a. \*  $P < 0.05$ , \*\*  $P < 0.01$ , \*\*\*  $P < 0.001$  versus WT; ##  $P < 0.01$ , ###  $P < 0.001$  versus Sham (Students'  $t$  test).





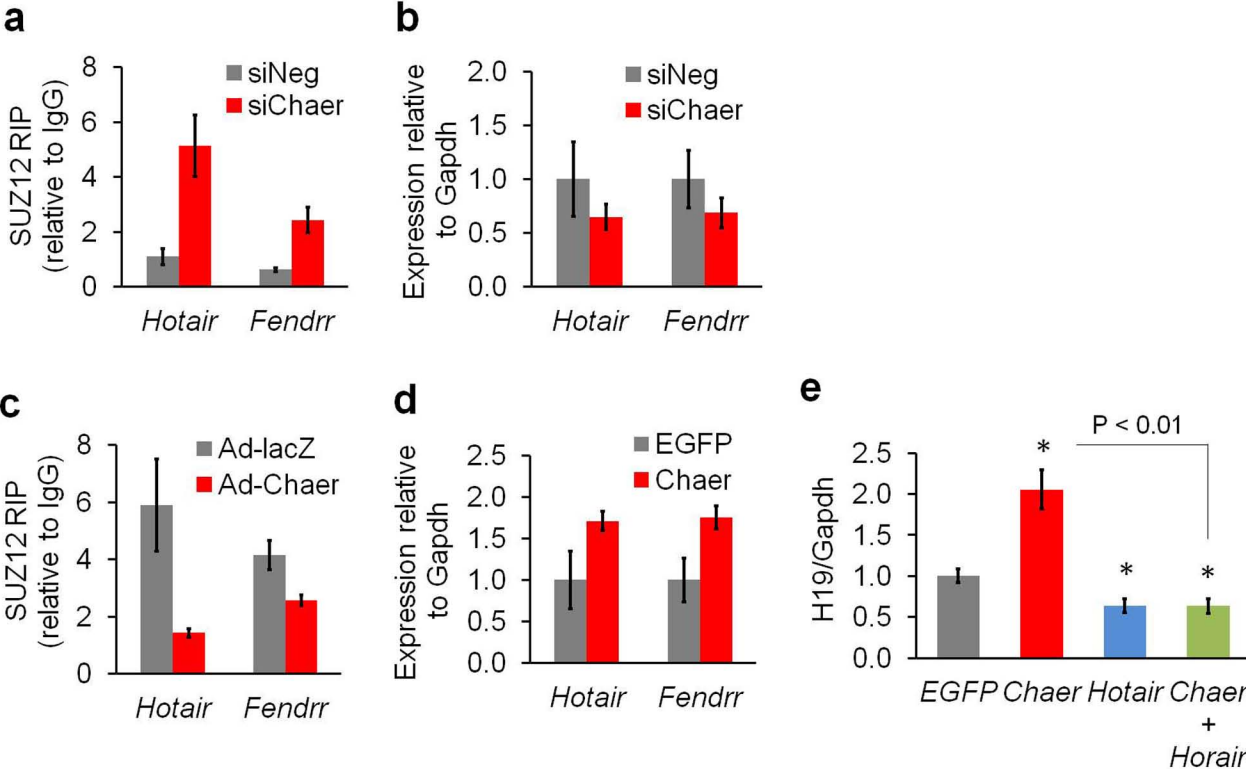
**Supplementary Figure 4. *Chaer* is both necessary and sufficient for the induction of hypertrophic genes.**

(a) Representative images of isolated neonatal rat ventricular myocytes (NRVMs) transfected with *Chaer*-specific siRNA (siChaer) or a negative control siRNA (siNeg) with or without hypertrophic stimulation by phenylephrine (PE, 50  $\mu$ M) from three independent experiments. (b) Representative images of NRVMs infected by adenoviruses expressing *Chaer* (Ad-*Chaer*) or lacZ (Ad-lacZ) from three independent experiments. Scale bars, 100  $\mu$ m. (c) *Chaer* knockdown in NRVMs significantly reduced the induction of hypertrophy genes including *Anf*, *Myh7* and *Acta1* after PE treatment without affecting its neighbor gene HOP domain protein (*Hopx*). Data were mean  $\pm$  s.e.m. n = 3. \*\*  $P < 0.01$  versus siNeg; ##  $P < 0.01$ , ###  $P < 0.001$  versus Control (Students' *t* test). (d) *Chaer* overexpression in NRVMs by Adenovirus significantly increased the expression of *Myh7* and *Acta1* without affecting *Anf* and *Hopx*. Data were mean  $\pm$  s.e.m. n = 3. \*  $P < 0.05$ , \*\*\*  $P < 0.001$  versus Ad-lacZ (Students' *t* test).



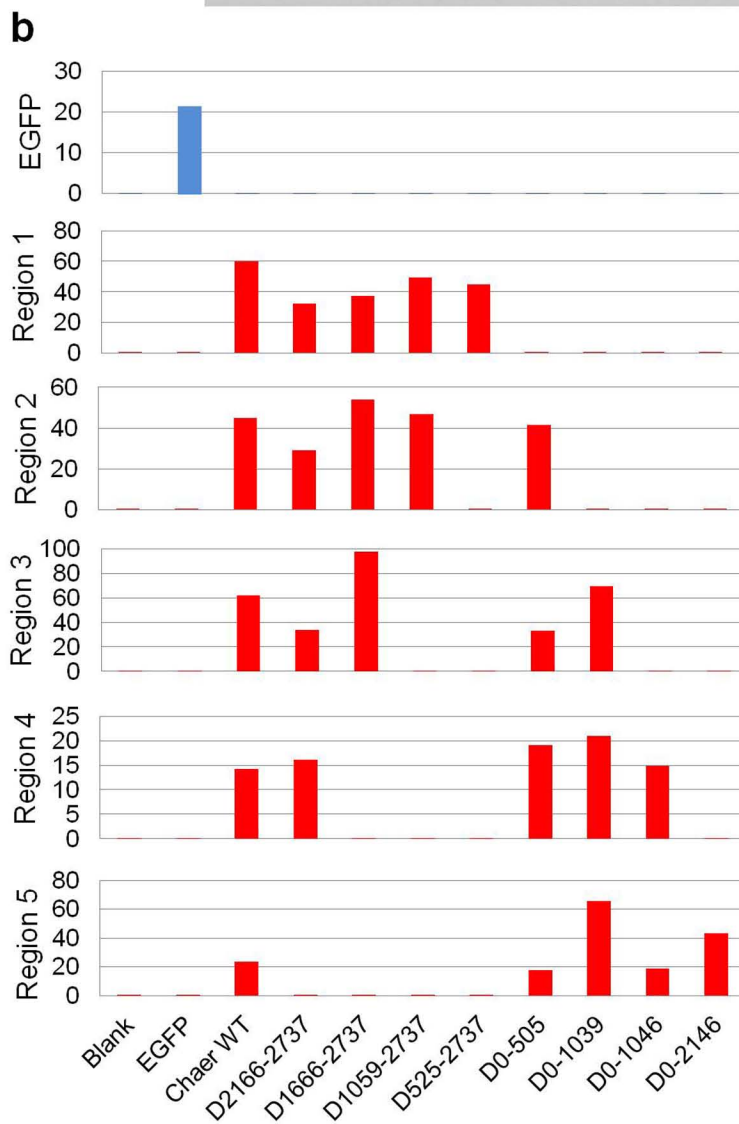
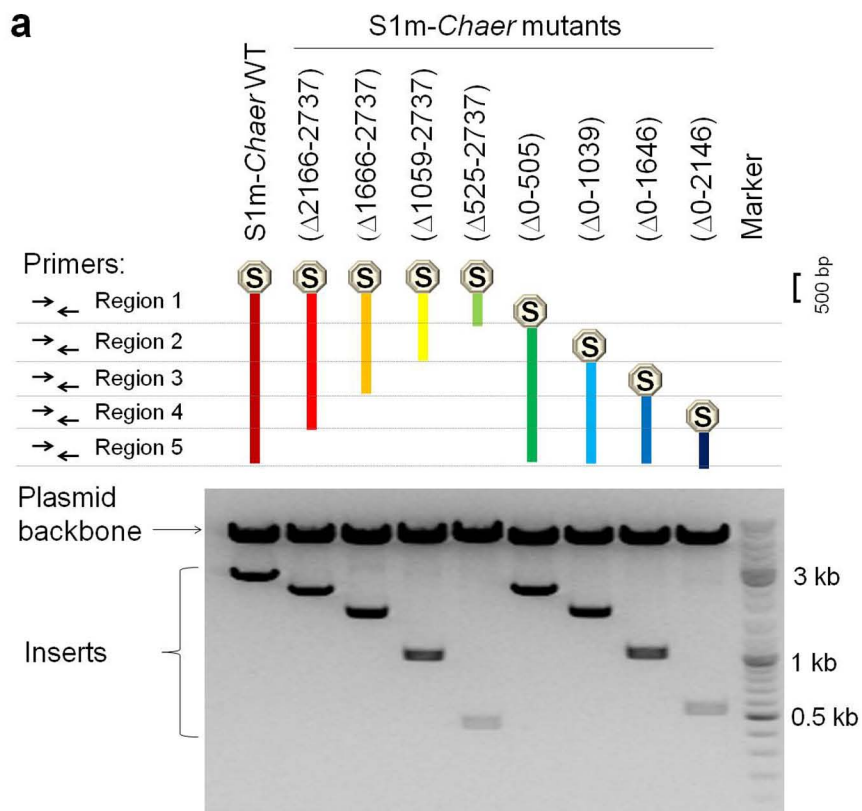
**Supplementary Figure 5. *Chaer* remodels global transcriptome reprogramming during cardiac hypertrophy independent of DNA methylation.**

(a) Heat map of the RNA sequencing data of NRVM transcriptome revealed that half of the genes regulated by phenylephrine (PE) were reversed by siRNA-mediated *Chaer* silence (left), and majority of the genes regulated by *Chaer* knockdown showed opposite regulation by PE treatment (right). siNeg, negative control siRNA; siChaer, *Chaer* specific siRNA. (b) Schematic of gene numbers in four different comparisons and negatively correlating genes shared by siNeg-PE/siNeg-control and siChaer-PE/siNeg-PE (upper), as well as by siChaer-control/siNeg-control and siChaer-PE/siChaer-control. (c) *Chaer* knockdown by siRNA suppressed *H19* expression in NRVMs with or without phenylephrine (PE, 50  $\mu$ M) treatment detected by real-time RT-PCR assay. Data were mean  $\pm$  s.e.m. n = 3. \*  $P < 0.05$  versus siNeg (Students'  $t$  test). (d) Adenovirus-mediated *Chaer* overexpression increased *H19* expression in NRVMs detected by real-time RT-PCR assay. Data were mean  $\pm$  s.e.m. n = 3. \*  $P < 0.05$  versus Ad-lacZ (Students'  $t$  test). (e) DNA methylation levels at *H19* promoter region in NRVMs transfected with siNeg or siChaer under PE treatment or non-treatment. DNA samples with and without AciII digestion (only cuts CCGC without methylation at CpG) from all groups were subjected to qRT-PCR to test three fragments covering the AciII sites at *H19* promoter region. Data were mean  $\pm$  s.d. from triplicates. (f) Immunoblotting analysis for histone methylations (H3K4me2, H3K9me2, H3K27me2, H3K27me3) and total H3 in PE-treated NRVMs treated at different time points (0, 24, 48 h).



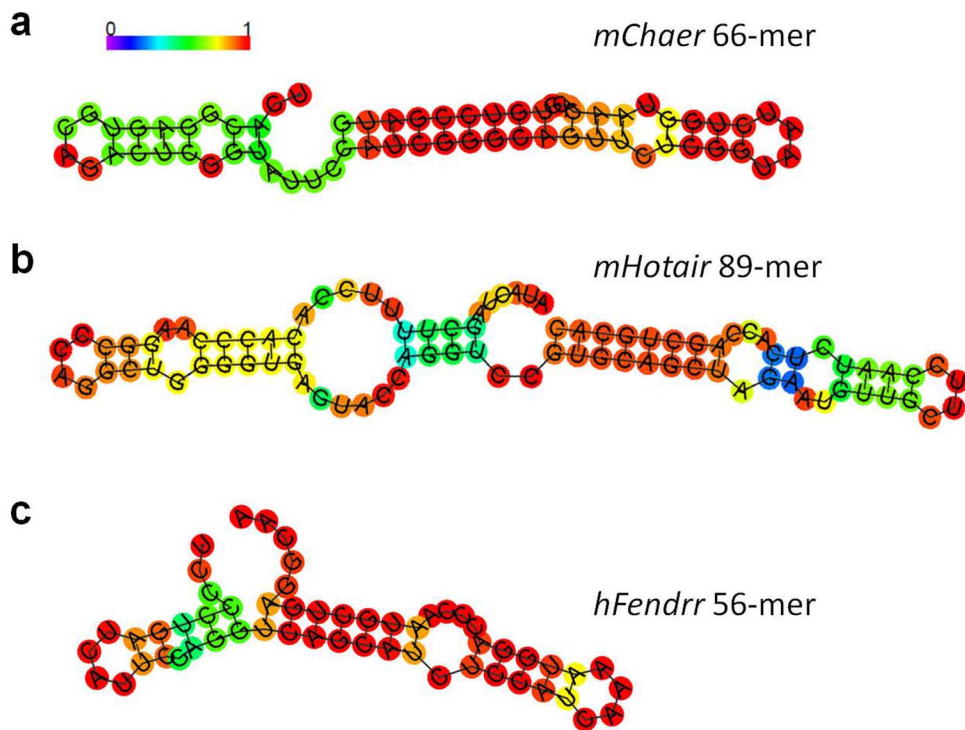
**Supplementary Figure 6. *Chaer* competes with PRC2-binding lncRNAs.**

(a) *Chaer* silence with specific siRNA enhanced PRC2 interaction with other lncRNAs (*Hotair* and *Fendrr*) in NRVMs. RNA immunoprecipitation (RIP) analysis was performed with SUZ12 antibody. Data were mean  $\pm$  s.d. from triplicates. (b) *Chaer* knockdown did not change the RNA expression levels of *Hotair* and *Fendrr*. (c) SUZ12 RIP analysis showing that *Chaer* overexpression in mouse embryonic fibroblasts (MEFs) suppressed PRC2 interaction with *Hotair* and *Fendrr*. (d) *Chaer* overexpression in MEFs did not change the RNA expression levels of *Hotair* and *Fendrr*. (e) Co-expression of *Hotair* abolished the increase of *H19* expression by *Chaer* overexpression in MEFs. Data were mean  $\pm$  s.e.m. n = 3. \*  $P < 0.05$ , \*\*  $P < 0.01$  versus corresponding siNeg, Ad-lacZ or EGFP controls (Students'  $t$  test).



**Supplementary Figure 7. Validation of the truncated *Chaer* mutations for tagged RNA pull-down assay.**

(a) *Chaer* mutations were truncated at roughly 500 bp from both 5' and 3' ends (schematic illustrated upper), and cloned into pcDNA5-CMV using BamHI and XhoI right behind a modified S1 tag (S1m). After amplification, the plasmids were double digested with BamHI/XhoI and separated on 1% agarose gel (lower). (b) Real-time RT-PCR with primers illustrated in (a) confirmed that all mutations were stably and evenly expressed in MEFs.



**d**

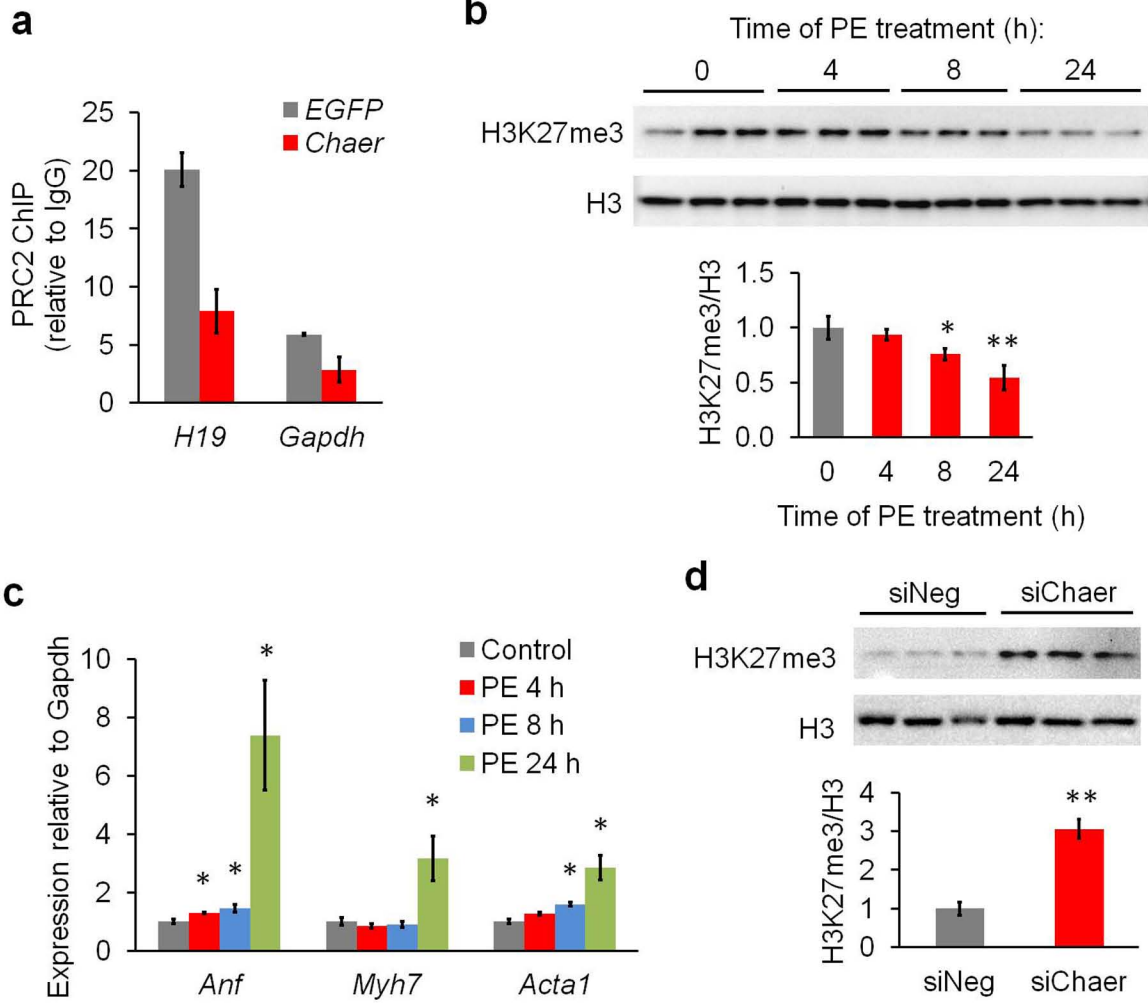
**Red: Interacting residues** **Blue: Non-interacting residues**

MGQTGKKSEKGPVCWRKRVKSEYMRLRQLKRFRRRADEVKTMFSSNRQKILERTETLNQEW  
 KQRRIQPVHIMTSVSSLRGTRECSVTSDLDFPAQVIPLKTLNAVASVPIMYSWSPLQQNF  
 MVEDETVLHNIPYMGDEVLDQDGTFFIELIKNYDGKVHGDRECGFINDEIFVELVNALGQ  
 YNDDDDDDGDDPDEREEKQKDLLEDNRDDKETCPPRKFPADKIFEAISSMFPDKGTAEEL  
 KEKYKELTEQQLPGALPPECTPNIDGPNKSVQREQSLHSFHTLFCRRCFKYDCFLHPPFH  
 ATPNTYKRKNTETALDNKPCGPQCYQHLEGAKEFAAALTAERIKTPPKRPGGRRRGRLPN  
 NSSRPSTPTISVLESKDTDSDREAGTETGGENNDKEEEEKDETSSSSEANSRCQTPIKM  
 KPNI~~EP~~PENVEWSGAEASMF~~R~~VLIGTYYDNFCAIARLIGTKTCRQVYEF~~R~~VK~~ES~~SIAPV  
 PTEDVDTPPRKKK~~R~~HRLWAAHCRKIQLKKDGSSNHVYNYQPCDHPRQPCDSSCPCVIAQ  
 NFCEKFCQCSSE~~C~~QNRFP~~G~~CRCKAQCN~~T~~KQCPCYLAVRECDPLCLTCGAADHWDSKNVS  
 CKNCSIQRGS~~K~~HLLAPSDVAGWGIFIKDPVQKNEFISEYCGEIIISQDEADRRGKVYDK  
 YMCSFLN~~L~~NDFVVDAT~~R~~KG~~N~~KIRFANHSVNPNCYAKVMMVNGDHRIGIFAKRAIQTGE  
 ELFFDYRYSQADALKYVGI~~R~~EMEIP



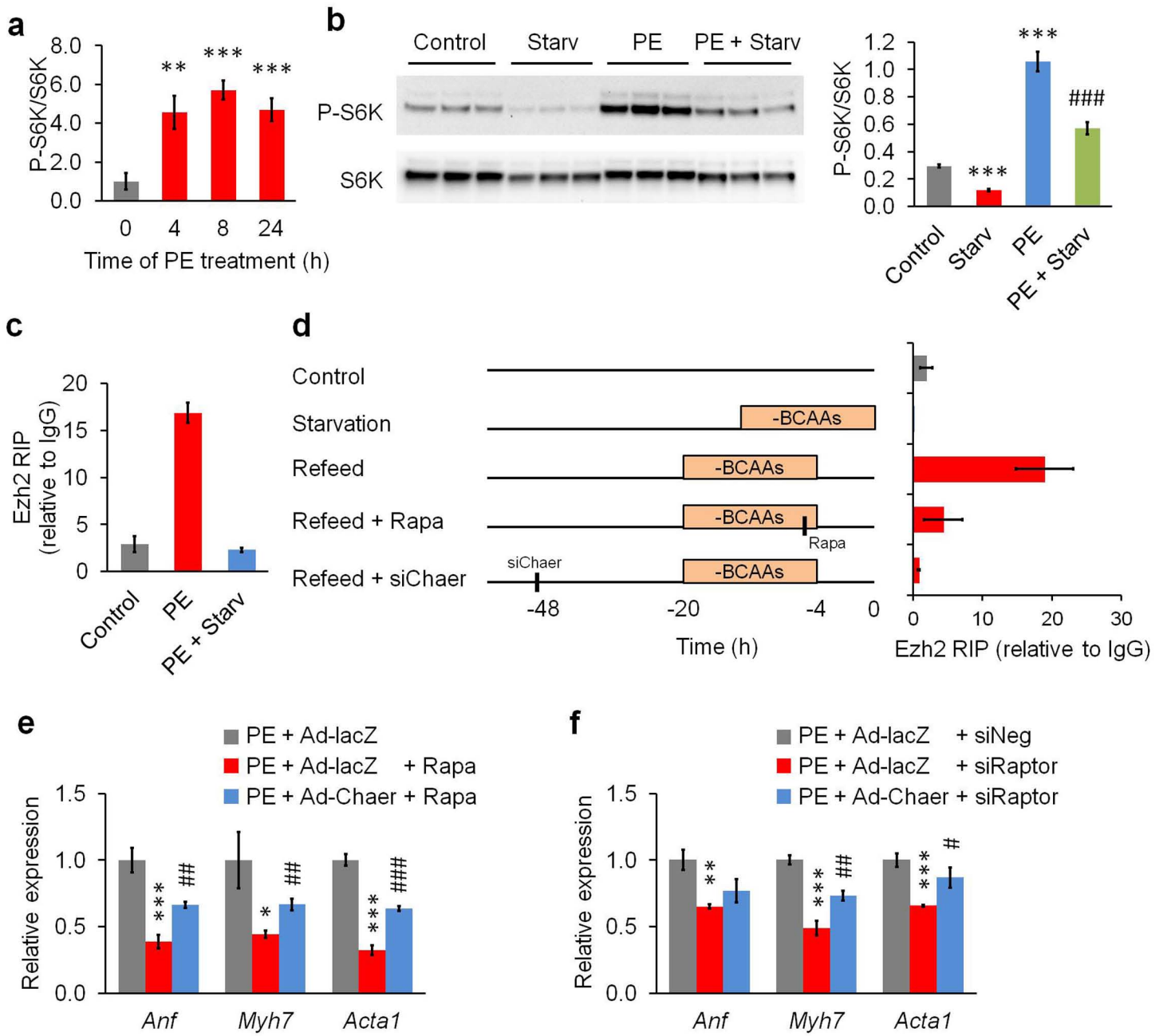
**Supplementary Figure 8. Sequence details underlying interaction between Ezh2 and lncRNAs.**

(a-c) RNA secondary structures of motifs from mouse *Chaer* (a), mouse *Hotair* (b) and human *Fendrr* (c) were predicted by RNAfold WebServer (<http://rna.tbi.univie.ac.at/cgi-bin/RNAfold.cgi>) based on minimum free energy (MFE) and partition function. Similar motifs with resemble stem-loop structures were identified among three lncRNAs. (d) Ezh2 RNA binding residues were predicted by RNA-Protein Interaction Prediction (RPIseq, <http://pridb.gdc.b.iastate.edu/RPISeq/>). Predicted interacting residues were labeled with red, whereas non-interacting residues were labeled with blue.



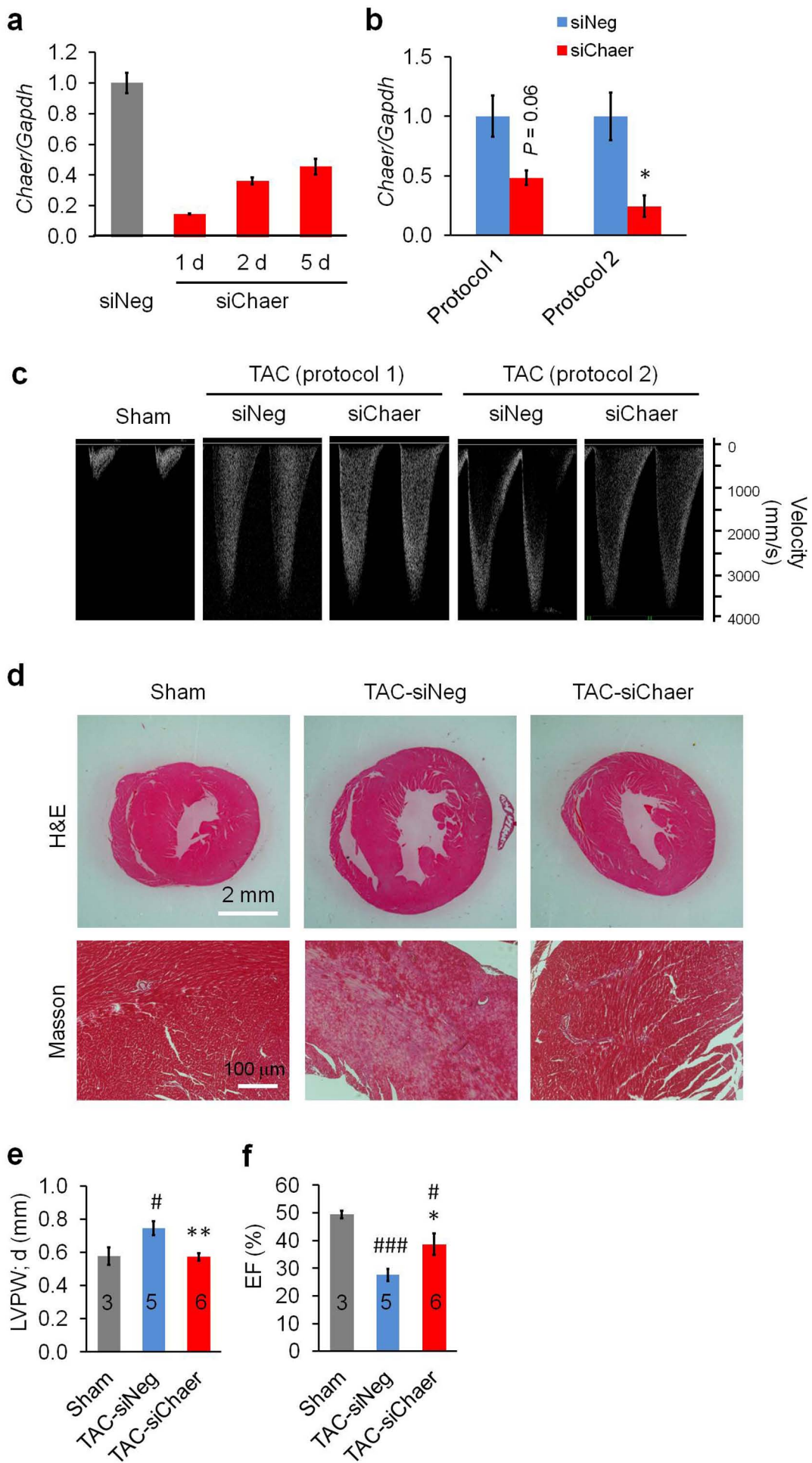
**Supplementary Figure 9. Correlation between histone methylation at H3K27 and hypertrophic gene induction in PE-induced cardiomyocyte hypertrophy.**

(a) Chromatin immuno-precipitation (ChIP) analysis with anti-Ezh2 antibody showing the PRC2 targeting to promoter regions of *H19* and *Gapdh* in MEFs expressing EGFP or *Chaer*. Data were mean  $\pm$  s.d. from triplicates. (b) PE treatment caused a gradual decrease of global H3K27me3 levels as early as 8 h after PE treatment. Data were mean  $\pm$  s.e.m. n = 3. \* $P < 0.05$ , \*\*  $P < 0.01$  versus 0 h of PE treatment (Students' *t* test). (c) Time-course of PE-induced expression of hypertrophic genes *Anf*, *Myh7* and *Acta1*. Data were mean  $\pm$  s.e.m. n = 3. \*  $P < 0.05$  versus Control (Students' *t* test). (d) *Chaer* silence with siRNA rescued the decreased global H3k27me3 levels in PE-treated NRVMs. Data were mean  $\pm$  s.e.m. n = 3. \*\*  $P < 0.01$  (Students' *t* test).



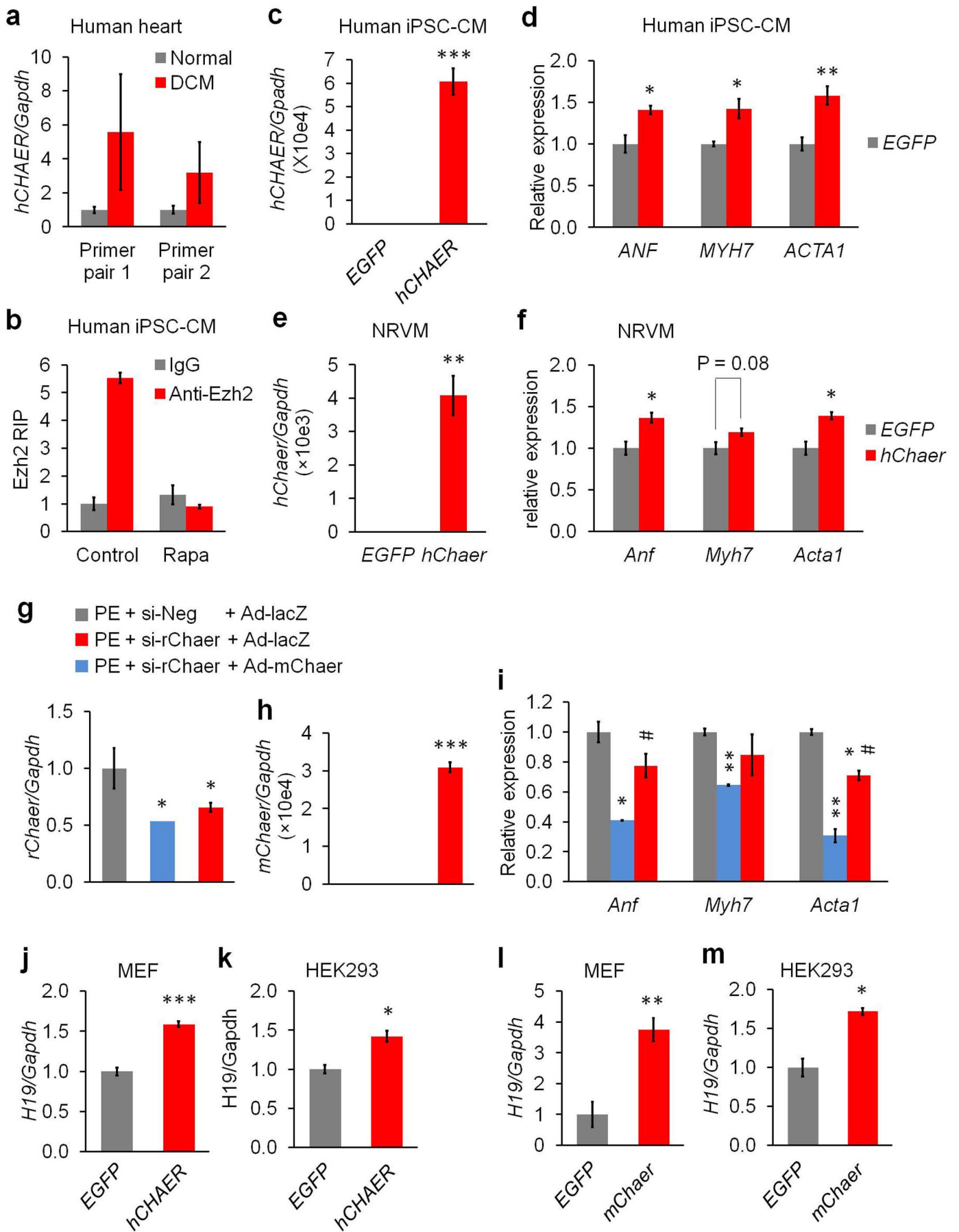
**Supplementary Figure 10. MTOR signaling pathway mediates the enhancement of *Chaer*-PRC2 interaction upon hypertrophy stimulation.**

(a) Analyzed data for mTOR downstream target S6K phosphorylation immuno-blot showed in **Figure 5a**. Data were mean  $\pm$  s.e.m.  $n = 3$ . \*\*  $P < 0.01$ , \*\*\*  $P < 0.001$  versus control (Students'  $t$  test). (b) Immuno-blot and analyzed data for S6K phosphorylation in NRVMs with and without starvation under control or PE treatment. Data were mean  $\pm$  s.e.m.  $n = 3$ . \*\*\*  $P < 0.001$  versus control; ###  $P < 0.001$  versus PE (Students'  $t$  test). (c) RIP analysis for *Chaer* with anti-Ezh2 antibody showing that starvation blocked PE-enhanced *Chaer*-PRC2 interaction. Data were mean  $\pm$  s.d. from triplicates. (d) Effects of BCAA starvation and refeeding NRVMs with or without rapamycin (Rapa) treatment or *Chaer* knockdown on *Chaer*-PRC2 interaction detected by Ezh2 RIP analysis. Timeline of treatments is schematically illustrated (left). Data were mean  $\pm$  s.d. from triplicates. (e,f) *Chaer* over-expression rescued the suppressed expression of *Anf*, *Myh7* and *Acta1* by Rapa (e) or siRaptor (f) in PE-treated NRVMs. Data were mean  $\pm$  s.e.m.  $n = 3$ . \* $p < 0.05$ , \*\* $p < 0.001$ , \*\*\* $p < 0.001$  versus PE controls; # $p < 0.05$ , ## $p < 0.01$ , ### $p < 0.001$  versus Ad-lacZ with Rapa or siRaptor (Students'  $t$  test).



**Supplementary Figure 11. Pre-empty knockdown of *Chaer in vivo* blocks pathological remodeling in TAC-induced hypertrophy.**

(a) Knockdown efficiency of nanoparticle-mediated transfection of siChaer in mouse hearts at 1, 2 and 5 days after injection. Data were mean  $\pm$  s.d. from triplicates (b) Validation of *Chaer* knockdown efficiency in both strategy 1 and 2 (**Fig. 6b**) by real-time RT-PCR. Data were mean  $\pm$  s.e.m. n = 3. \*p < 0.05 versus siNeg (Students' *t* test). (c) TAC surgery caused even acceleration of the blood velocity within the banding site of aorta in all groups evaluated by Echocardiography at pulsed-wave color Doppler mode. (d) Pre-empty knockdown of *Chaer in vivo* prevented the progression of fibrosis measured by Masson tri-chrome staining. (e-f) In addition to heart weight/body weight ratio, siChaer injection before TAC (protocol 1) significantly reduced LV posterior wall thickness at diastole (LVPW; d) (e) and preserved the ejection fraction (EF) (f) evaluated by Echocardiography. Data were mean  $\pm$  s.e.m. Sample numbers were labeled on bars. \*p < 0.05, \*\*p < 0.01 versus siNeg; #p < 0.05, ###p < 0.001 versus Sham (Students' *t* test).





**Supplementary Figure 12. Conservation of *Chaer* function in mouse, rat and human cells.**

(a) Expression of human *CHAER* (*hCHAER*) homolog in patient hearts with dilated cardiomyopathy (DCM) measured by real-time RT-PCR using two pairs of primers targeting human *CHAER*. Data were mean  $\pm$  s.e.m. n = 4. (b) RNA immunoprecipitation (RIP) assay with anti-Ezh2 antibody measuring its binding with *hCHAER* homolog in induced pluripotent stem cell-derived cardiomyocytes (iPSC-CM) with or without Rapamycin (inhibitor of mTOR signaling; 20 nM) treatment. Data were mean  $\pm$  s.d. from triplicates. (c,d) Effects of *hCHAER* overexpression using nanoparticle-mediated transfection (c) on the mRNA levels of hypertrophic genes *Anf*, *Myh7* and *Acta1* in iPSC-CMs (d). Data were mean  $\pm$  s.e.m. n = 3. \**P* < 0.05, \*\**P* < 0.01 versus EGFP (Students' *t* test). (e,f) Effects of *hCHAER* overexpression using nanoparticle-mediated transfection (e) on the mRNA levels of hypertrophic genes *Anf*, *Myh7* and *Acta1* in neonatal rat ventricular myocytes (NRVMs) (f). Data were mean  $\pm$  s.e.m. n = 3. \**P* < 0.05, \*\**P* < 0.01 versus EGFP (Students' *t* test). (g-i) Overexpression of mouse *Chaer* (*mChaer*) with Adenovirus (h) in NRVMs with rat *Chaer* (*rChaer*) knockdown (g) rescued the suppression on PE-induced expression of *Anf*, *Myh7* and *Acta1* (i). Data were mean  $\pm$  s.e.m. n = 3. \**P* < 0.05, \*\**P* < 0.01, \*\*\**P* < 0.001 versus PE + siNeg + Ad-lacZ; #*P* < 0.05 versus PE + si-rChaer + Ad-lacZ (Students' *t* test). (j,k) Effects of *hCHAER* overexpression on *H19* expression in MEFs (j) and HEK293 cells (k). Data were mean  $\pm$  s.e.m. n = 3. \**P* < 0.05, \*\*\**P* < 0.001 versus EGFP (Students' *t* test). (l,m) Effects of *mChaer* overexpression on *H19* expression in MEFs (l) and HEK293 cells (m). Data were mean  $\pm$  s.e.m. n = 3. \**P* < 0.05, \*\*\**P* < 0.001 versus EGFP (Students' *t* test).